IEEE Access
Multidisciplinary | Rapid Review | Open Access Journal

Received September 20, 2019, accepted September 27, 2019, date of publication October 4, 2019,
date of current version October 17, 2019.

Digital Object Identifier 10.1109/ACCESS.2019.2945568

Upgrading of the Existing Bi-Pole to the New Four-Pole Back-to-Back HVDC Converter for Greater Reliability and Power Quality

SABAH RAMADHAN MOHAMMED, JIASHEN TEH, (Member, IEEE), AND MOHAMAD KAMAROL, (Senior Member, IEEE)
School of Electrical and Electronic Engineering, Universiti Sains Malaysia, Nibong Tebal 14300, Malaysia
Corresponding author: Mohamad Kamarol (eekamarol@usm.my)

This work was supported in part by the Universiti Sains Malaysia through the Bridging Grant under Grant 304.PELECT.6316098.

ABSTRACT Back-to-back high-voltage direct current systems are used to transfer electrical power between two asynchronous AC systems. The existing bi-pole back-to-back system (2PBTBS) can be converted into the four-pole back-to-back system (4PBTBS) to save in the required infrastructure for proposed installations. This upgrading provides four parallel 12-pulse DC circuits instead of only two 12-pulse DC circuits as in the existing 2PBTBS. The power transfer capability of each DC circuit in the proposed system is 25% of the original system capacity instead of 50% as in the existing 2PBTBS. The reliability of the proposed 4PBTBS is improved twice, and the line-to-line DC voltage levels are reduced to 50% in comparison with the existing 2PBTBS. In this study, the 4PBTBS and existing 2PBTBS are simulated using MATLAB/Simulink. Simulation result shows that the proposed 4PBTBS has four parallel 12-pules DC circuits at lower line-to-line DC voltage and higher power quality compared with the existing 2PBTBS. These results validate the performance of the proposed system obtained from upgrading the existing 2PBTBS.

INDEX TERMS LCC-HVDC transmission, back-to-back HVDC system, reliability, 6-pulse HVDC converter, 12-pulse HVDC converter.

I. INTRODUCTION

This paper is an extension of the work originally presented in the 2018 IEEE PES Asia-Pacific Power and Energy Engineering Conference [1]. The back-to-back system (BTBS) indicates that the converter sides (rectifier and inverter) of the high-voltage direct current (HVDC) transmission are interconnected directly by short bus-bars. The whole system is located in the same building, usually in the same thyristor valve hall, and controlled by the same controller. In the absence of HVDC transmission lines, such as the case of a BTBS, the line losses are not considered, and the design of the BTBS HVDC project is economically achieved at relatively low DC voltage levels and high DC current associated [2], [3].

The BTBS is used to tie two asynchronous AC systems (systems that are not in synchronism). These two AC systems can be of different operating frequencies, such as one 50 Hz and the other 60 Hz or the same operating frequencies [4]–[6]. The HVDC links listed in reference [7] installed throughout the world by Siemens Company show examples of AC systems that may not be synchronized with their neighboring. A BTBS HVDC offers a practical solution to interconnect these nonsynchronous AC systems [8].

The one-pole back-to-back system (1PBTBS) is typically designed for single 12-pulse DC circuit operation. Given their low cost, 1PBTBSs are widely used in existing BTBS projects [9, 10]. The disadvantage of the 1PBTBS (one 12-pulse DC circuit) is that if one 6-pulse bridge of 12-pulse DC circuit falls, then the entire system becomes completely lost. The parallel interconnection of two or more 1PBTBSs is used to increase the reliability and capacity of electrical energy exchanging between two AC systems [11], [12]. For example, the Vyborgskaya BTBS project consists of four 1PBTBS units, with each unit rated at 355 MW. This project provides an asynchronous connection between the AC power systems of Russia and Finland [13]. The most common topology for existing BTBS is the 2PBTBS, which is parallel of two 1PBTBSs, each of which can be operated independently; if one 1PBTBS is on maintenance or on the outage, then the other 1PBTBSs can operate as a single 12-pulse DC circuit

The associate editor coordinating the review of this manuscript and approving it for publication was Derek Abbott.

TABLE 1. Operating modes of the existing 2PBTBS.

SC%	CC1%	CC2%	Operating modes
100	50	50	Normal state
50	0	50	Mono-pole-outage (a)
50	50	0	Mono-pole-outage (b)
0	0	0	Bi-pole outage

where, SC=System Capacity, CC= Circuit Capacity
(a) One or more six-pulse bridge(s) in CC1 in outage.
(b) One or more six-pulse bridge(s) in CC2 in outage.

with 50% of the total system capacity [14]. The drawback of the existing 2PBTBS is that if two of the 6-pulse bridges in different 12-pulse DC circuits fail, then the entire system becomes completely lost.

A novel four-pole HVDC power transmission topology is presented in [15] to increase reliability and power density transmission. The application of the proposed four-pole system in [15] is limited to the Point-to-Point HVDC transmission system without using the ground electrode for carrying its return current. This study introduces a novel topology based on [15] for Back-to-Back HVDC system applications. This topology is proposed to upgrade an existing 2PBTBS LCC-HVDC with two parallel 12-pulse DC circuits to the 4PBTBS with four parallel 12-pulse DC circuits for increased system reliability. In this paper, the operational concepts of the proposed system are illustrated, and the differences between the proposed system and the existing 2PBTBS are analyzed. For system performance testing, the simulation models of 4PBTBS and 2PBTBS are performed in MATLAB/Simulink.

II. OPERATIONAL CONCEPTS OF THE PROPOSED 4PBTBS

A. EXISTING 2PBTBS AND PROPOSED 4PBTBS CONFIGURATIONS

An existing 2PBTBS is shown in Fig. 1(a) consisting of four 6-pulse rectifier bridges $Y1\_R, D1\_R, Y2\_R, D2\_R$ and four 6-pulse inverter bridges $Y1\_I, D1\_I, Y2\_I, D2\_I$. Each 6-pulse bridge converter (rectifier or inverter) is connected to an AC system through a three-phase transformer. Transformers $Yg/Y1$ and $Yg/Y2$ are connected in wye-grounded/wye, and transformers $Yg/D1$ and $Yg/D2$ are connected in wye-grounded/delta to provide a 30° phase shift necessary for 12-pulse converter operation to enable partial harmonic cancellations on the AC and DC sides. The DC side of each serial connection of two 6-pulse bridges operates as single 12-pulse converters on each side, which are $Y1\_R, D1\_R$ and $Y2\_R, D2\_R$ on the rectifier side and $Y1\_I, D1\_I$ and $Y2\_I, D2\_I$ on the inverter side. Then, these 12-pulse converters (rectifiers and inverters) are coupled only by a short bus-bars $+L1$, $-L2$, $-L3$, $+L4$. This setup of the existing 2PBTBS has two independent 12-pulse DC circuits (1PBTBS). Each 1PTBTS is capable of 50% of the total system capacity. Table 1 shows the operating modes of the existing 2PBTBS topology.

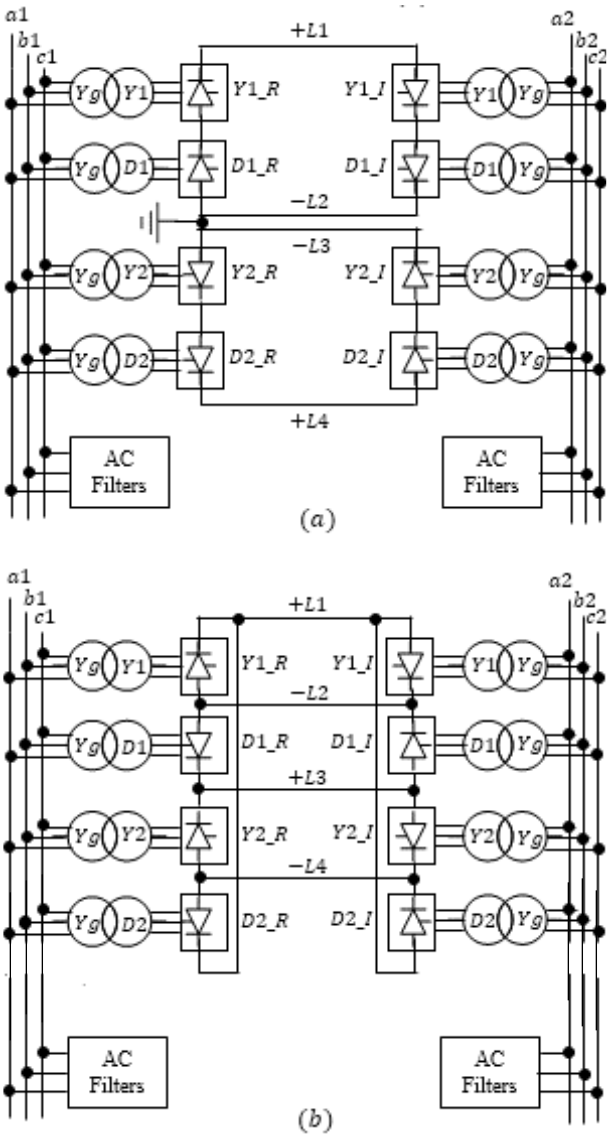

FIGURE 1. Topologies of the LCC HVDC, (a) existing 2PBTBS, (b) proposed 4PBTBS.

Furthermore, each serial connection of the two 6-pulse converters at the rectifier and inverter sides is operating as a 12-pulse DC circuit with 50% of the total system capacity:

1) Circuit 1 comprises ($Y1\_R$ and $D1\_R$) on the rectifier side and ($Y1\_I$ and $D1\_I$) on the inverter side. These 6-pulse bridges are coupled by two short bus-bars $+L1$ and $-L2$.
2) Circuit 2 comprises ($Y2\_R$ and $D2\_R$) on the rectifier side and coupled with ($Y2\_I$ and $D2\_I$) on the inverter side by short bus-bars $-L3$ and $+L4$.

The proposed 4PBTBS is created by the following connection: (1) Two-positive polarity 6-pulse rectifier bridges $Y1\_R, D2\_R$ with two-negative polarity six-pulse inverter bridges $Y1\_I, D2\_I$ through a short bus-bar at $L1$. (2) Two-positive polarity six-pulse rectifier bridges $D1\_R, Y2\_R$ with two-negative polarity six-pulse inverter bridges $D1\_I, Y2\_I$

through a short bus-bar at $L3$. (3) Two-negative polarity six-pulse rectifier bridges $Y1\_R, D1\_R$ with two-positive polarity six-pulse inverter bridges $Y1\_I, D1\_I$ through a short bus-bar at $L2$. (4) Two-negative polarity six-pulse rectifier bridges $Y2\_R$, $D2\_R$ with two-positive polarity six-pulse inverter bridges $Y2\_I, D2\_I$ through a short bus-bar at $L4$. This setup provides four parallel independent DC circuits (loop currents). Each loop current is capable of 25% of the system capacity.

Furthermore, each serial connection of the two 6-pulse converters at the rectifier and inverter sides is operating as a 12-pulse DC circuit:

1) Circuit 1 comprises two six-pules bridges ($Y1\_R$ and $D1\_R$) on the rectifier side and coupled with two six-pulse bridges ($Y1\_I$ and $D1\_I$) on the inverter side by short bus-bars $+L1$, $-L2$ and $+L3$.
2) Circuit 2 comprises ($D1\_R$ and $Y2\_R$) on the rectifier side and coupled with ($D1\_I$ and $Y2\_I$) on the inverter side by short bus-bars $-L2$, $+L3$ and $-L4$.
3) Circuit 3 comprises ($Y2\_R$ and $D2\_R$) on the rectifier side and coupled with ($Y2\_I$ and $D2\_I$) on the inverter side by short bus-bars $+L3$, $-L4$ and $+L1$.
4) Circuit 4 comprises ($D2\_R$ and $Y1\_R$) on the rectifier side and coupled with ($D2\_I$ and $Y1\_I$) on the inverter side by short bus-bars $-L4$, $+L1$ and $-L2$.

This setup provides four parallel 12-pulse DC circuits. Each 12-pulse DC circuit is capable of 50% of the system capacity. Table 2 shows the operating modes of the 4PBTBS topology.

TABLE 2. Operating modes of the proposed 4PBTBS.

SC%	CC1%	CC2%	CC3%	CC4%	Operating modes
100	25	25	25	25	Normal state
50	0	0	25	25	Bi-pole-outage (a)
50	25	0	0	25	Bi-pole-outage (b)
50	25	25	0	0	Bi-pole-outage (c)
50	0	25	25	0	Bi-pole-outage (d)
0	0	0	0	0	Four-pole-outage

where, SC=System Capacity, CC= Circuit Capacity
(a) CC1 and CC2 are in outage mode simultaneously.
(b) CC2 and CC3 are in outage mode simultaneously.
(c) CC3 and CC4 are in outage mode simultaneously.
(d) CC4 and CC1 are in outage mode simultaneously.

B. DC VOLTAGE AND CURRENT PARAMETERS IN THE EXISTING 2PBTBS AND THE PROPOSED 4PBTBS

Fig. 2(a and b) shows the equivalent circuit of 2PBTBS and 4PBTBS during steady-state operation, respectively. In the figures, V_{Y1_R}, V_{D1_R}, V_{Y2_R}, V_{D2_R} and V_{Y1_I}, V_{D1_I}, V_{Y2_I}, V_{D2_I} are DC voltages of the 6-pulse rectifier and inverter bridges, respectively. In Fig. 2(a), i_{d1}, i_{d2} are the DC currents of loops 1 and 2, respectively. In Fig. 2(b),i_{d1}, i_{d2}, i_{d3}, i_{d4} are the DC line currents of short bus-bars $+L1$, $-L2$, $-L3$, $+L4$, respectively. i_{Y1}, i_{D1}, i_{Y2}, i_{D2} are the respective DC currents of 6-pulse bridges $Y1\_R$, $D1\_R$, $Y2\_R$, $D2\_R$ at the rectifier side and $Y1\_I$, $D1\_I$, $Y2\_I$, $D2\_I$ at the inverter side.

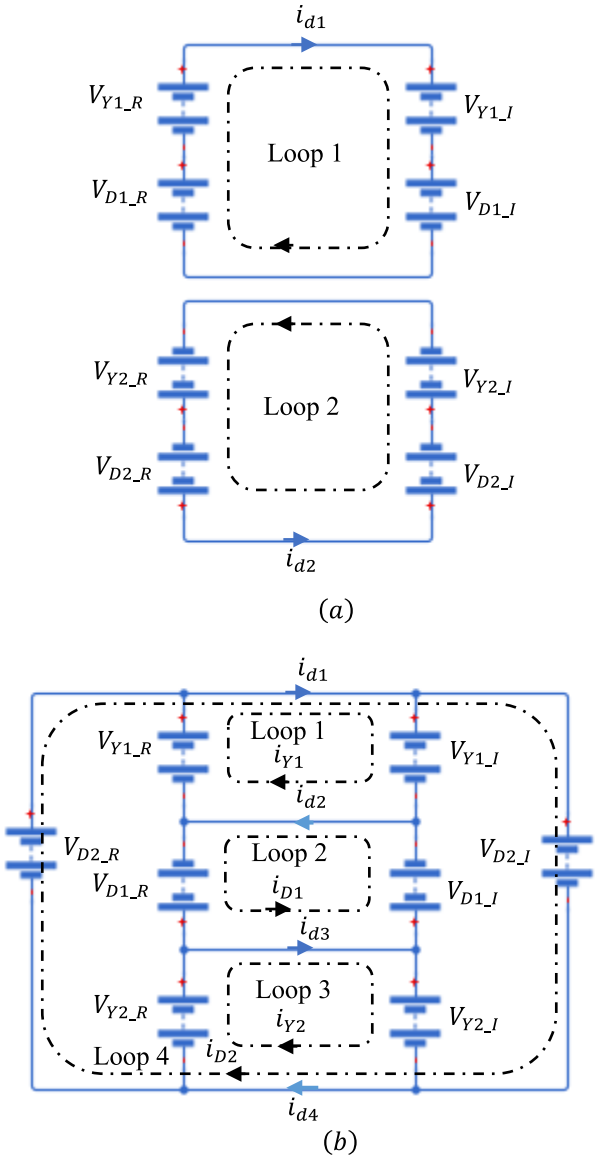

FIGURE 2. Equivalent circuit of LCC HVDC back-to-back systems, (a) existing 2PBTBS, (b) proposed 4PBTBS.

By apply mesh analysis for each loop current (12-pulse DC circuit) of the 2PBTBS in Fig. 2(a) is shown as follows:

$$+V_{D1\_R} + V_{Y1\_R} - V_{Y1\_I} - V_{D1\_I} = 0 \quad \text{forloop1}$$
$$+V_{Y2\_R} + V_{D2\_R} - V_{D2\_I} - V_{Y2\_I} = 0 \quad \text{forloop2}$$

By contrast, apply mesh analysis for each loop current of the 4PBTBS in Fig. 2(b) is shown as follows:

$$+V_{Y1\_R} - V_{Y1\_I} = 0 \quad \text{for loop1}$$
$$+V_{D1\_R} - V_{D1\_I} = 0 \quad \text{for loop2}$$
$$+V_{Y2\_R} - V_{Y2\_I} = 0 \quad \text{for loop3}$$
$$+V_{D2\_R} - V_{D2\_I} = 0 \quad \text{for loop4}$$

Let V_{d_R} and V_{d_I} be the corresponding values of the DC voltages of 6-pulse rectifier and inverter bridges for the 2PBTBS

and 4PBTBS.

$$\left.\begin{array}{ll} V_{Y1\_R}=V_{D1\_R}=V_{Y2\_R}=V_{D2\_R}=V_{d\_R} & \text{rectifier side} \\ V_{Y1\_I}=V_{D1\_I}=V_{Y2\_I}=V_{D2\_I}=V_{d\_I} & \text{inverter side} \end{array}\right\} \quad (1)$$

By substituting Equation (1) into loop currents in the 2PBTBS and 4PBTBS, the DC voltages of each 12-pulse converter unit are:

$$\left.\begin{array}{ll} 2V_{d\_R}=2V_{d\_I} & \text{for loop 1 in 2PBTBS} \\ 2V_{d\_R}=2V_{d\_I} & \text{for loop 2 in 2PBTBS} \end{array}\right\} \quad (2)$$

$$\left.\begin{array}{ll} V_{d_R}=V\_d_R & \text{for loop 1 in 4PBTBS} \\ V_{d_R}=V\_d_R & \text{for loop 2 in 4PBTBS} \\ V_{d_R}=V\_d_R & \text{for loop 3 in 4PBTBS} \\ V_{d_R}=V\_d_R & \text{for loop 4 in 4PBTBS} \end{array}\right\} \quad (3)$$

where $2V_{d\_R}, 2V_{d\_I}$ in Equation (2) for the 2PBTBS and V_{d_R}, V_{d_I} in Equation (3) for the 4PBTBS represent the DC voltage of 12-pulse converter at the rectifier and inverter sides, respectively. Therefore, considering Equations (1) to (3), the DC voltage of each 12-pulse converter unit of the 4PBTBS is only half of that in the 2PBTBS.

The same current flows through each 6-pulse bridge unit in the 2PBTBS and 4PBTBS can be expressed as

$$i_d = \begin{cases} i_{d1}=i_{d2} & \text{for 2 PBTBS} \\ i_{Y1}=i_{D1}=i_{Y2}=i_{D2} & \text{for 4 PBTBS} \end{cases} \quad (4)$$

The main difference between the conventional 2PBTBS and proposed 4PBTBS configurations is in the 2PBTBS connection. The 6-pulse bridge and 12-pulse converter currents are identical ($i_{d1}=i_{d2}=i_d$). The ratio of DC voltage of the 12-pulse converter to the 6-pulse bridge is twice. By contrast, in the 4PBTBS connection, the 6-pulse bridge and 12-pulse converter DC voltages are identical. According to Kirchhoff's current law, the algebraic sum of currents in and out of each a bus-bar at any instant is

$$\left.\begin{array}{ll} i_{d1}=i_{Y1}+i_{D2}=2i_d & \text{for busbar } +\text{L1} \\ i_{d2}=i_{Y1}+i_{D1}=2i_d & \text{for busbar } -\text{L2} \\ i_{d3}=i_{D1}+i_{Y2}=2i_d & \text{for busbar } +\text{L3} \\ i_{d4}=i_{Y2}+i_{D2}=2i_d & \text{for busbar } -\text{L4} \end{array}\right\}. \quad (5)$$

The ratio of DC current of 12-pulse converter to 6-pulse bridge is twice. The DC current and voltage parameters of mathematical analysis results for the 2PBTBS and 4PBTBS are summarized in Table 3.

TABLE 3. DC current and voltage parameters for comparison between 2PBTBS and 4PBTBS.

Parameters	2PBTBS	4PBTBS
6-pulse bridge DC voltage in *pu*	1	1
6-pulse bridge DC current in *pu*	1	1
12-pulse bridge DC voltage in *pu*	2	1
12-pulse bridge DC current in *pu*	1	2
Number of parallel loop current per system	2	4
Number of 6-pulse bridge unit per system	8	8

C. HVDC POWER TRANSFER CAPABILITIES AND POWER LOSSES

In general, the 6-pulse bridge units of HVDC systems (1PBTBS, 2PBTBS, and 4PBTBS) have similar components and can be acted as a rectifier or an inverter [4], [16]. Thus, the following equations are addressed:

$$\begin{aligned} V_{Y1\_R} &= V_{D1\_R}=V_{Y2\_R}=V_{D2\_R} \\ &= \left(3\sqrt{2}/\pi\right) V_{LL}\cos\left(\alpha_R\right) - R_{C\_R} i_d \end{aligned} \quad (6)$$

$$\begin{aligned} V_{Y1\_I} &= V_{D1\_I}=V_{Y2\_I}=V_{D2\_I} \\ &= \left(3\sqrt{2}/\pi\right) V_{LL}\cos\left(180^\circ-\alpha_I\right) + R_{C\_I} i_d \end{aligned} \quad (7)$$

where V_{LL} is the line-to-line AC voltage (in rms), i_d is the DC current, and α_R, α_I are the firing angles of the 6-pulse rectifier and inverter bridges, respectively. $R_{c\_R}i_d$ and $R_{c\_I}i_d$ in Equations (6) and (7) represent the voltage drop due to a three-phase transformer leakage inductance [16].

By substituting Equations (6) and (7) into loop currents for the 2PBTBS and 4PBTBS, the total power transfer and power losses of the six-pulse rectifier and inverter bridges in the existing 2PBTBS and the proposed 4PBTBS can be calculated as

$$\begin{aligned} P_{2\text{PBTBS}} &= \sum_{k=1,2,\ldots,n}^{n}\left[2\left(3\sqrt{2}/\pi\right)V_{LL}\cos(\alpha_R) i_d - 2i_d^2 R_{c\_R}\right]_k \\ &= \sum_{k=1,2,\ldots,n}^{n}\left[2\left(3\sqrt{2}/\pi\right) V_{LL}\cos\left(180^\circ - \alpha_I\right) i_d + 2i_d^2 R_{c\_I}\right]_k \end{aligned} \quad (8)$$

$$\begin{aligned} P_{4\text{PBTBS}} &= \sum_{k=1,2,\ldots,n}^{n}\left[\left(3\sqrt{2}/\pi\right)V_{LL}\cos(\alpha_R) i_d - i_d^2 R_{c\_R}\right]_k \\ &= \sum_{k=1,2,\ldots,n}^{n}\left[\left(3\sqrt{2}/\pi\right) V_{LL}\cos\left(180^\circ - \alpha_I\right) i_d + i_d^2 R_{c\_I}\right]_k \end{aligned} \quad (9)$$

where $P_{2\text{PBTBS}}, P_{4\text{PBTBS}}$ are the total power capacity in the 2PBTBS and the 4PBTBS, respectively. n is the loop current number. n is equal to 2 and 4 for Equations (8) and (9), correspondingly. The $\left(3\sqrt{2}/\pi\right) V_{LL}\cos\left(\alpha_R\right) i_d$ at the rectifier and $\left(3\sqrt{2}/\pi\right) V_{LL}\cos\left(180^\circ-\alpha_I\right) i_d$ at the inverter is power capacity per 6-pulse bridge unit. $i_d^2 R_{c\_R}$ and $i_d^2 R_{c\_I}$ are 6-pulse bridge losses for the rectifier and the inverter, respectively.

III. SIMULATION AND RESULTS

A. EXISTING 2PBTBS AND PROPOSED 4PBTBS DESCRIPTION

A 2000 MW 4PBTBS HVDC system simulation model performed in MATLAB/SIMULINK is implemented to verify the feasibility and success of the upgrading of the existing 2PBTBS into new 4PBTBS. This procedure aims to demonstrate the performance of the 4PBTBS in managing the power flow between two asynchronous AC systems and investigating failure effects of the 12-pulse DC circuit as shown in Tables 1 and 2 on the reliability of the entire system. By contrast, the existing 2PBTBS simulation with the same power is used in this simulation in addition to the standard

reference for the comparison. In this simulation, the normal state and mono-pole outage (b) as in Table 1 are taken as examples for the 2PBTBS operating modes. The normal state and bi-pole outage (c) as in Table 2 are taken as examples for 4PBTBS operating modes. Furthermore, the simulation operates in systems 2PBTBS and 4PBTBS simultaneously from $t = 0$ to 1 s in normal state mode and from $t = 1$ s to 2 s in outage modes.

TABLE 4. Circuit parameters for the simulation model.

AC Parameters		AC system 1	AC system 2	
Short circuit level (MVA)		20000	40000	
Base AC power (VA 3-phase) (MVA)		3000	3000	
Nominal voltage (kV)		500	345	
Transformer primary voltage (kV)		500	345	
Transformer secondary voltage (kV)		200	200	
Transformer nominal power (MVA)		600	600	
Transformer leakage inductance (Ω)		$R_{c\_R} = 10.2$	$R_{c\_I} = 10.2$	
Number of transformers required		8	8	
AC filters	11th tuned filter (MVAR)	300	300	
	13th tuned filter (MVAR)	300	300	
	High order filter (MVAR)	300	300	
	Capacitor bank (MVAR)	300	300	
Frequency (f) (Hz)		60	50	
Power factor cos φ		0.89	0.89	
Back-to-back HVDC System Parameters			**2PS**	**4PS**
Number of six-pulse bridge required			8	8
Number of short bus-bar			4	4
Nominal DC power (MW)			2000	2000
Line-to-line DC voltage (kV)			1000	250
Nominal DC voltage line-to-neutral (kV)			500	250
Nominal six-pulse bridge DC voltage (kV)			250	250
Nominal 12-pulse bridge DC voltage (kV)			500	250
Nominal six-pulse bridge DC current (kA)			2	2
DC line current (kA)			2	4

Note: all AC voltages are Line-to-Line (rms)

Fig. 3(a and b) demonstrates the simulation model of the 2PBTBS and 4PBTBS interconnection systems, correspondingly. In this simulation, the rectifier side (for 2PBTBS and 4PBTBS) is connected to AC system 1 through busbar B_{rec} (Fig. 3). The inverter side (for the 2PBTBS and 4PBTBS) is connected to AC system 2 through busbar B_{inv} (Fig. 3). The parameters are detailed in Table 4. The 2PBTBS and 4PBTBS configurations use the same 6-pulse bridge units and the same AC filters. The 4PBTBS is modified on the basis of [17]. The power losses per 6-pulse bridge (rectifier or inverter) in the proposed 4PBTBS and the existing 2PBTBS are also simulated in terms of the voltage drop in equivalent commutation resistance R_{c_R} and R_{c_I} at each converter transformer at the rectifier and inverter sides, respectively. The simulation model of the 2PBTBS and 4PBTBS also adopts the same control modes as [17] with the modification on the rectifier and inverter controls for the 4PBTBS control. Thus, at the rectifier side of the 4PBTBS, the rectifier controls the currents $i_{d1}, i_{d2}, i_{d3}, i_{d4}$ at reference current i_{d_ref}. At the inverter side of the 4PBTBS, the inverter controls the voltages $V_{Y1}, V_{D1}, V_{Y2}, V_{D2}$ and currents $i_{d1}, i_{d2}, i_{d3}, i_{d4}$ at reference voltage V_{d_ref} and reference current i_{d_ref}, respectively. In the conventional 2PBTBS, the master control has four operating modes, which is shown in Table 1. In the proposed 4PBTBS, the master control has six operating modes, which is shown in Table 2.

B. OPERATING MODES

Figure 4 presents the simulation results for verifying the operating modes of the rectifier and inverter sides for the existing 2PBTBS (Fig. 3(a)). By contrast, Fig. 5 presents the simulation results for verifying the operating modes of the rectifier and inverter sides for the proposed 4PBTBS (Fig. 3(b)).

In this simulation (2PBTBS and 4PBTBS), all 6-pulse bridges on the rectifier and inverter sides are enabled by the master control, and the power transfer is initialized by ramping the currents at $t = 0.3$ s. The 2PBTBS DC line currents i_{d1}, i_{d2} and the 4PBTBS DC line currents $i_{d1}, i_{d2}, i_{d3}, i_{d4}$ start to build-up, and the line-to-ground DC voltages V_{d12}, V_{d23} in the 2PBTBS and the line-to-line DC voltages $V_{d12}, V_{d23}, V_{d34}, V_{d41}$ in the 4PBTBS are charged at its nominal values at 1 pu (1 pu = 500 kV) and 1 pu (1 pu = 250 kV), respectively. At $t = 0.4$ s, the DC line currents i_{d1}, i_{d2} in the 2PBTBS and the DC line currents $i_{d1}, i_{d2}, i_{d3}, i_{d4}$ in the 4PBTBS are ramped to 1 pu and 2 pu (1 pu = 2 kA), respectively, in 0.18 s.

At time $t = 1$ s, permanent outage pole(s) DC faults are applied at 6-pulse bridge $Y2\_R, D2\_R$ in the 2PBTBS and 4PBTBS. In the 2PBTBS, the master control blocks 6-pulse bridges $Y2\_R, D2\_R, Y2\_I, D2\_I$ in DC circuit 2 to allow the healthy parts of DC circuit 1 in the 2PBTBS to operate as 1PBTBS. By contrast, the master control in the 4PBTBS blocks 6-pulse bridges $Y2\_R, D2\_R, Y2\_I, D2\_I$ to allow the healthy parts of circuits 1 and 2 in the 4PBTBS to operate as 2PBTBS. The DC currents in the healthy parts of the 2PBTBS and 4PBTBS reach steady-state at 0.58 s to 1.4 s. At 1.4 s, the stop sequence is initiated by ramping down the currents to zero. At 1.7 s, the pulses from the master control block the healthy 6-pulse bridges on the rectifier and inverter sides in the 2PBTBS and 4PBTBS.

The waveform of AC voltages V_{a1}, V_{b1}, V_{c1}, line currents i_{a1}, i_{b1}, i_{c1}, total AC active power P_1 and reactive power Q_1 are measured through busbar B_{rec} at AC system 1, as shown in Fig. 4(a–c) for the 2PBTBS and Fig. 5(a–c) for the 4PBTBS, respectively. The measurement shows that the active and reactive powers are 1 pu (1 pu = 2000 MW) and 0.4 pu (1 pu = 2000 MVAR) for the 2PBTBS, respectively, whereas the active and reactive powers for the 4PBTBS are 1 pu and 0.4 pu, respectively. At time $t = 1$ s to 1.6 s, Fig. 4(b and c) for the 2PBTBS and Fig. 5(b and c) for the 4PBTBS show results when the AC powers and AC currents are initiated ramping down from 1 pu to 0.5 pu during monopolar and bipolar outage mode operations, respectively. Positive active and reactive powers indicate that the rectifier sides in the 2PBTBS (Fig. 4(c)) and 4PBTBS (Fig. 5(c)) draw active power from AC system 1.

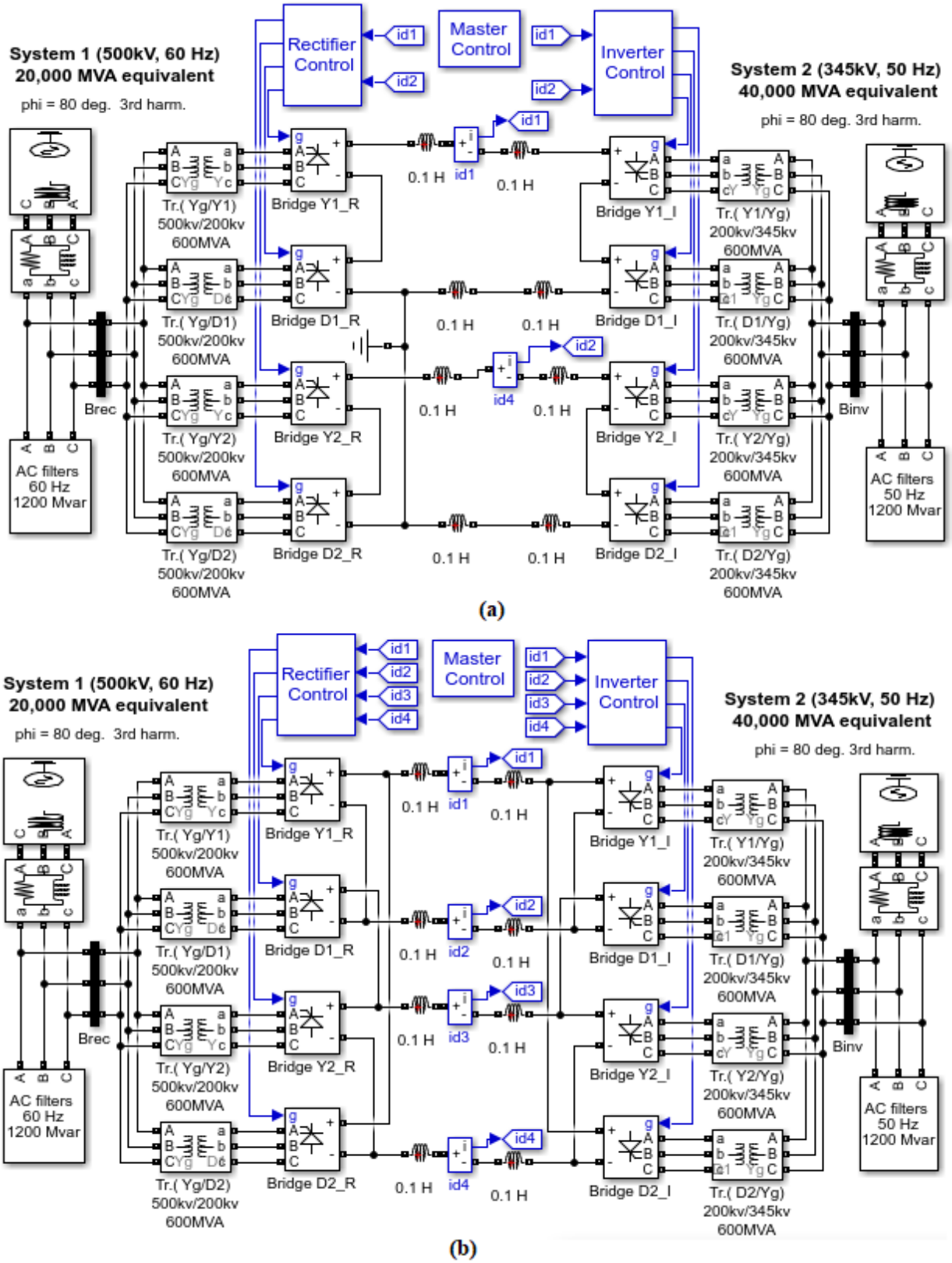

FIGURE 3. MATLAB/SIMULINK software simulation model of, (a) existing 2PBTBS, (b) proposed 4PBTBS.

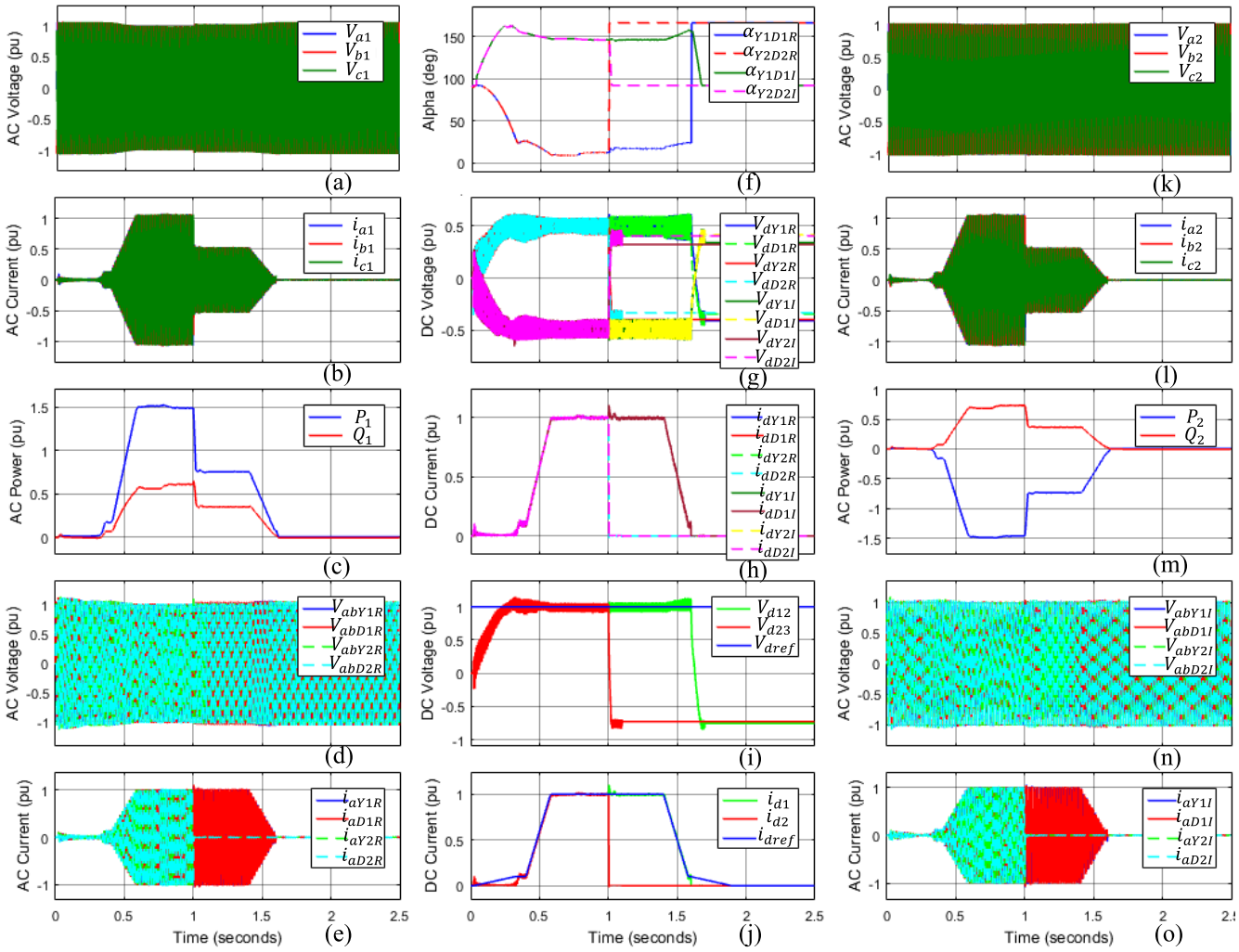

FIGURE 4. Waveforms for the conventional 2PBTBS: (a) line-to-line AC voltages at AC system 1, (b) AC line currents at AC system 1, (c) active and reactive powers at AC system 1, (d) line-to-line AC voltages V_{ab} at each secondary-transformer at rectifier side, (e) AC phase currents i_a at each secondary-transformer at rectifier side, (f) Rectifier and Inverter alpha degrees, (g) DC 6-pulse bridge voltages, (h) DC 6-pulse bridge currents, (i) DC line-to-neutral voltages, (j) DC line currents, (k) line-to-line AC voltages at AC system 2, (l) AC line currents at AC system 2, (m) active and reactive powers at AC system 2, (n) line-to-line AC voltages V_{ab} at each secondary-transformer at inverter side, (o) AC phase currents i_a at each secondary-transformer at inverter side.

The waveform of AC voltages V_{a2}, V_{b2}, V_{c2}; line currents i_{a2}, i_{b2}, i_{c2}; total AC active power P_2; and reactive power Q_2 are measured through busbar B_{inv} at AC system 2, as shown in Fig. 4(k–m) and Fig. 5(k–m) for the 2PBTBS and 4PBTBS, respectively. The active and reactive powers are -1 pu (1 pu = 2000 MW) and 0.5 pu (1 pu = 2000 MVAR) for the 2PBTBS, whereas the active and reactive powers are -1 pu and 0.5 pu for the 4PBTBS, respectively. At time t = 1 s to 1.6 s, Fig. 4(l and m) for the 2PBTBS and Fig. 5(l and m) for the 4PBTBS show results when the AC powers (active and reactive) and AC currents are initiated ramping down from 100% to 50% during monopolar and bipolar outage mode operation, respectively. Negative active power indicates that the inverter sides in the 2PBTBS (Fig. 4(m)) and 4PBTBS (Fig. 5(m)) deliver active power to AC system 2. Positive reactive power indicates that the inverter sides in the 2PBTBS (Fig. 4(c and m)) and 4PBTBS (Fig. 5(c and m)) absorb reactive power from AC systems.

Fig. 4(d and e) and Fig. 4(n and o) for 2PBTBS show the line-to-line AC voltage and phase current at secondary winding for each transformer at the rectifier and inverter sides. At the rectifier side, the phase a to phase b voltages and phase a currents are 1 pu (1 pu = 200 kV) and 1 pu (1 pu = 500 MVA/200 Kv), respectively. At the inverter side, the phase a to phase b voltages and phase a currents are 1 pu (1 pu = 200 kV) and 1 pu (1 pu = 500 MW/200 kV), respectively. Fig. 5(d and e) and Fig. 5(n and o) depict the same results for the 4PBTBS. Both systems use the same transformer units. At time t =1 s to 1.6 s, Fig. 4(e and o) at the rectifier and inverter sides, respectively, for the 2PBTBS show result when the AC currents i_{aY2R}, i_{aD2R} and i_{aY2I}, i_{aD2I} are initiated ramping down from 1 pu to

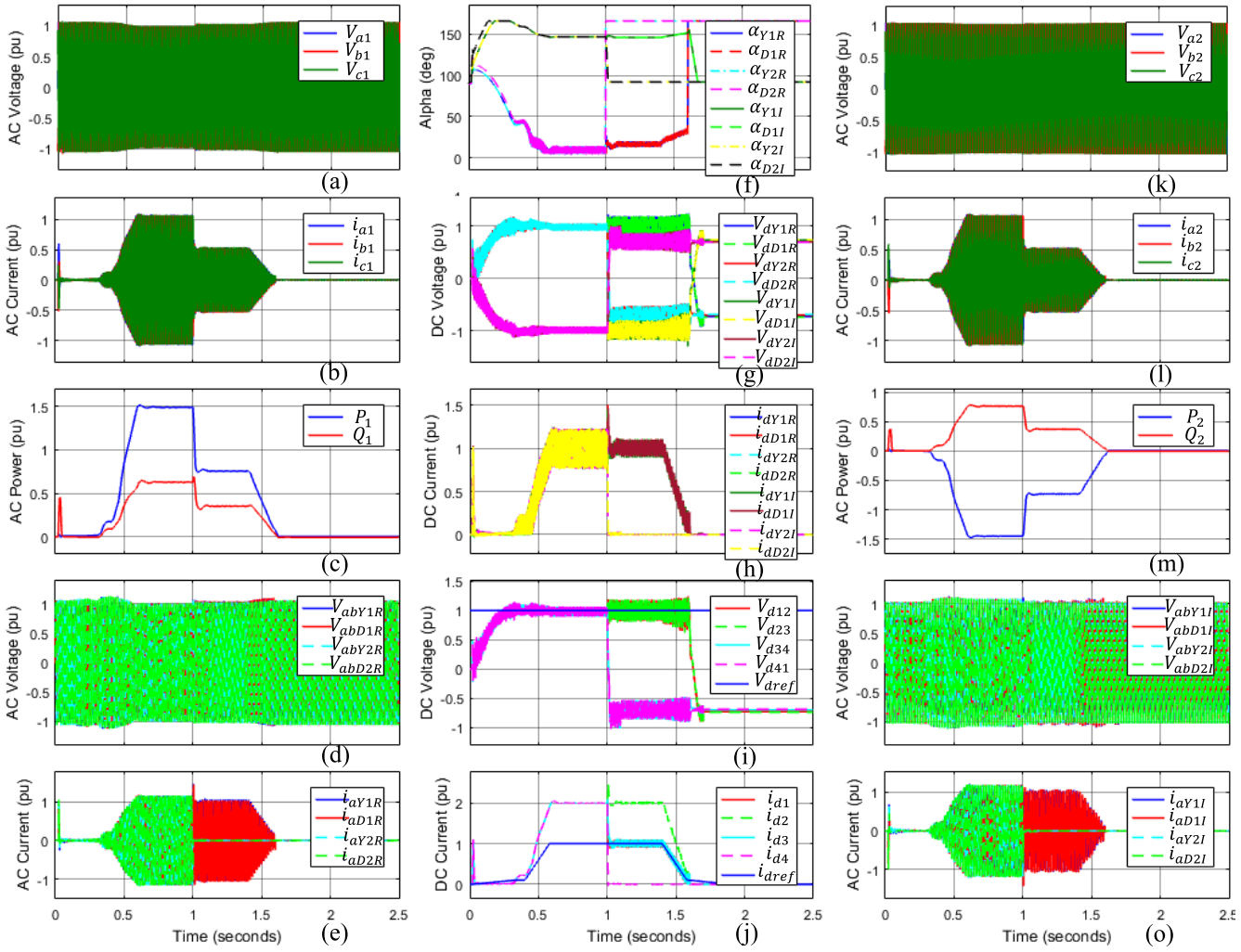

FIGURE 5. Waveforms for the proposed 4PBTBS: (a) line-to-line AC voltages at AC system 1, (b) AC line currents at AC system 1, (c) active and reactive powers at AC system 1, (d) line-to-line AC voltages V_{ab} at each secondary-transformer at rectifier side, (e) AC phase currents i_a at each secondary-transformer at rectifier side, (f) Rectifier and Inverter alpha degrees, (g) DC 6-pulse bridge voltages, (h) DC 6-pulse bridge currents, (i) DC line-to-line voltages, (j) DC line currents, (k) line-to-line AC voltages at AC system 2, (l) AC line currents at AC system 2, (m) active and reactive powers at AC system 2, (n) line-to-line AC voltages V_{ab} at each secondary-transformer at inverter side, (o) AC phase currents i_a at each secondary-transformer at inverter side.

zero during monopolar mode operation. By contrast, at time $t = 1$ s to 1.6 s, Fig. 5(e and o) at the rectifier and inverter sides, respectively, for 4PBTBS show result when the AC currents i_{aY2R}, i_{aD2R} and i_{aY2I}, i_{aD2I} are initiated ramping down from 1 pu to zero during bi-pole mode operation.

The 2PBTBS and 4PBTBS have used the same 6-pulse bridge units. Figs. 4(g) and 5(g) illustrate the same results for the 4PBTBS and 2PBTBS, respectively. As shown in Fig. 4(g) and 5(g), the DC voltages V_{Y1R}, V_{D1R}, V_{Y2R}, V_{D2R} have the same values at 0.5 pu at the rectifier side, whereas the DC voltages $V_{Y1I}, V_{D1I}, V_{Y2I}, V_{D2I}$ have similar values at -0.5 pu at the inverter side. In addition, Figs. 4(g) and 5(g) show that the DC voltages of the faulty 6-pulse bridges are initiated ramping down from 1 pu to zero during monopolar and bipolar outage mode operations.

Fig. 4(h) for the 2PBTBS and Fig. 5(h) for the 4PBTBS display the currents at the positive terminal of 6-pulse converters. The result shows the DC currents $i_{Y1R}, i_{D1R}, i_{Y2R}, i_{D2R}, i_{Y1I}, i_{D1I}, i_{Y2I}, i_{D2I}$ have similar values at 1 pu. In addition, Figs. 4(h) and 5(h) show that the DC currents of the faulty 6-pulse bridges are initiated ramping down from 1 pu to zero during monopolar and bipolar outage mode operations.

For the 2PBTBS, Fig. 4(i) exhibits the line-to-neutral DC voltages V_{d12}, V_{d23}, and Fig. 4(j) exhibits the DC line currents i_{d1}, i_{d2}. These voltages track the reference voltage V_{d_ref} at 1 pu, and the currents track the reference current i_{d_ref} at 1 pu. Fig. 4(f) illustrates the firing angles $\alpha_{Y1D1R}, \alpha_{Y2D2R}$ at the rectifier side and $\alpha_{Y1D1I}, \alpha_{Y2D2I}$ at the inverter side of 12-pulse DC circuits. At the steady-state

between 0.58 and 1 s, the firing angles of the 12-pulse rectifier and inverter converters are 18° and 148°, respectively.

By contrast, for the 4PBTBS, Fig. 5(i) exhibits the line-to-line DC voltages V_{d12}, V_{d23}, V_{d34}, V_{d41} and Fig. 4(j) exhibits the DC line currents i_{d1}, i_{d2}, i_{d3}, i_{d4}. These voltages track the reference voltage V_{d_ref} at 1 pu, and currents also track the reference current i_{d_ref} at 1 pu. Fig. 5(f) illustrates the firing angles α_{Y1R}, α_{D1R}, α_{Y2R}, α_{D2R} at the rectifier side and α_{Y1I}, α_{D1I}, α_{Y2I}, α_{D2I} at the inverter side of 12-pulse DC circuits. At the steady-state between 0.58 and 1 s, the firing angles of the 12-pulse rectifier and inverter are 18° and 148°, respectively. Simulation results show that the proposed 4PBTBS can produce four parallel 12-pulse DC circuits at lower line-to-line DC voltage and higher DC current associated in comparison with the existing 2PBTBS. In addition, the simulation results show that the power capacity of each 12-pulse DC circuit in the 2PBTBS and 4PBTBS are 50% and 50% of the total system capacity, respectively. The main similarities/differences between the existing 2PBTBS and the proposed 4PBTBS simulation results as shown in Figs. 4 and 5 during normal state mode operation are listed in Table 5.

TABLE 5. Main similarities / differences between the 2PBTBS and 4PBTBS simulation results.

Main Similarities		
Parameters	**2PBTBS**	**4PBTBS**
Line-to-line AC voltage at AC system 1	500 kV	500 kV
Line-to-line AC voltage at AC system 2	345 kV	345 kV
AC line current at AC system 1	4 kA	4 kA
AC line current at AC system 2	5797 A	5797 A
Active AC power at AC system 1	2000 MW	2000 MW
Active AC power at AC system 2	-2000 MW	-2000 MW
Reactive AC power at AC system 1	800 MVAR	800 MVAR
Reactive AC power at AC system 2	1000 MVAR	1000 MVAR
Line-to-line AC voltage at each rectifier	200 kV	200 kV
Line-to-line AC voltage at each inverter	200 kV	200 kV
DC voltage per 6-pulse rectifier bridge	250 kV	250 kV
DC voltage per 6-pulse inverter bridge	-250 kV	-250 kV
DC current per 6-pulse rectifier bridge	2 kA	2 kA
DC current per 6-pulse inverter bridge	2 kA	2 kA
Total DC power capacity per system	2000 MW	2000 MW
DC power capacity per 6-pulse bride unit	500 MW	500 MW
Main Differences		
Parameters	**2PBTBS**	**4PBTBS**
Number of 12-pulse DC circuit	2	4
Line-to-line DC voltage per 12-pulse DC circuit	500 kV	250 kV
Line DC current per 12-pulse circuit	2 kA	4 kA
Power capacity per 12-pulse DC circuit per system	1000 MW	500 MW

The 2PBTBS and 4PBTBS have used the same components with their parameters. Therefore, Fig. 4 (a), (b), (c), (d), (e), (g), (k), (l), (m), (n), and (o) and Fig. 5 (a), (b), (c), (d), (e), (g), (k), (l), (m), (n), and (o) illustrate the same results for the 4PBTBS and 2PBTBS, respectively. The 2PBTBS and 4PBTBS topologies using the same 6-pulse bridge units (Fig. 1) and each 6-pulse bridge unit have the same parameters, as shown in Table 4. This result indicates that the line-to-line DC voltage of the 4PBTBS is only half of that in the 2PBTBS. The line DC current of the 4PBTBS is two times higher than that of the 2PBTBS.

The success of upgrading the existing 2PBTBS (Fig. 1(a)) to the new 4PBTBS HVDC converter (Fig. 1(b)) has been defined by the simulation results in Figs. 4 and 5, respectively. The 4PBTBS simulation results show that the waveforms do not exceed the voltage stresses and current capacity for an extended period in comparison with the existing 2PBTBS.

IV. POWER QUALITY

A. CHARACTERISTIC HARMONICS

In the HVDC converters, the harmonic generation is related to its pulse number. Therefore, the relation between the pulse number and the harmonic order on the AC and DC sides of the HVDC converter is given by [4].

$$h = \begin{cases} kp \pm 1 & \text{on AC side} \\ kp & \text{on DC side} \end{cases} \tag{10}$$

where h is the harmonic order, p is the pulse number of the HVDC converter, and k is the positive integer.

Total harmonic distortion (THD) is used to define the effect of the harmonics generated by 6-pulse or higher converter on the current at the AC system. It is expressed in the following equation [18]:

$$\text{THD} = \left[\left(\sqrt{\sum_{h=2}^{25} I_h^2} \right) \Big/ I_d \right] \times 100, \tag{11}$$

where I_h is the harmonic current of order h and I_d is the fundamental current.

The harmonics in AC line currents results under 12-pulse system operation in the 2PBTBS and 4PBTBS are shown in Table 6. These results are obtained from the Fast Fourier Transform (FFT) analysis tool in the MATLAB simulation model (Fig. 3) under normal state operation. Table 6 shows the relationship between the 12-pulse HVDC converter and the harmonics involved in AC line currents at AC systems 1 and 2 at bus-bars B_{rec} at the rectifier side and B_{inv} at the inverter side of 2PBTBS and 4PBTBS (Fig. 3). From the comparison of these two systems, we can conclude that each DC circuit in the existing 2PBTBS and the proposed 4PBTBS are constructed as 12-pulse systems. Table 6 shows that the THD in the phase a currents at AC systems 1 and 2 in the 2PBTBS are 6.90% and 8.22%, respectively. The THD values of the phase a currents at AC systems 1 and 2 in the 4PBTBS are 5.82% and 6.81%, respectively. The THD of the line currents at AC systems 1 and 2 of the proposed 4PBTBS has been reduced by approximately 1.08% and 1.41%, respectively, in comparison with the existing 2PBTBS. The THD values of the proposed 4PBTBS are the values specified in the IEEE 519 standard [18].

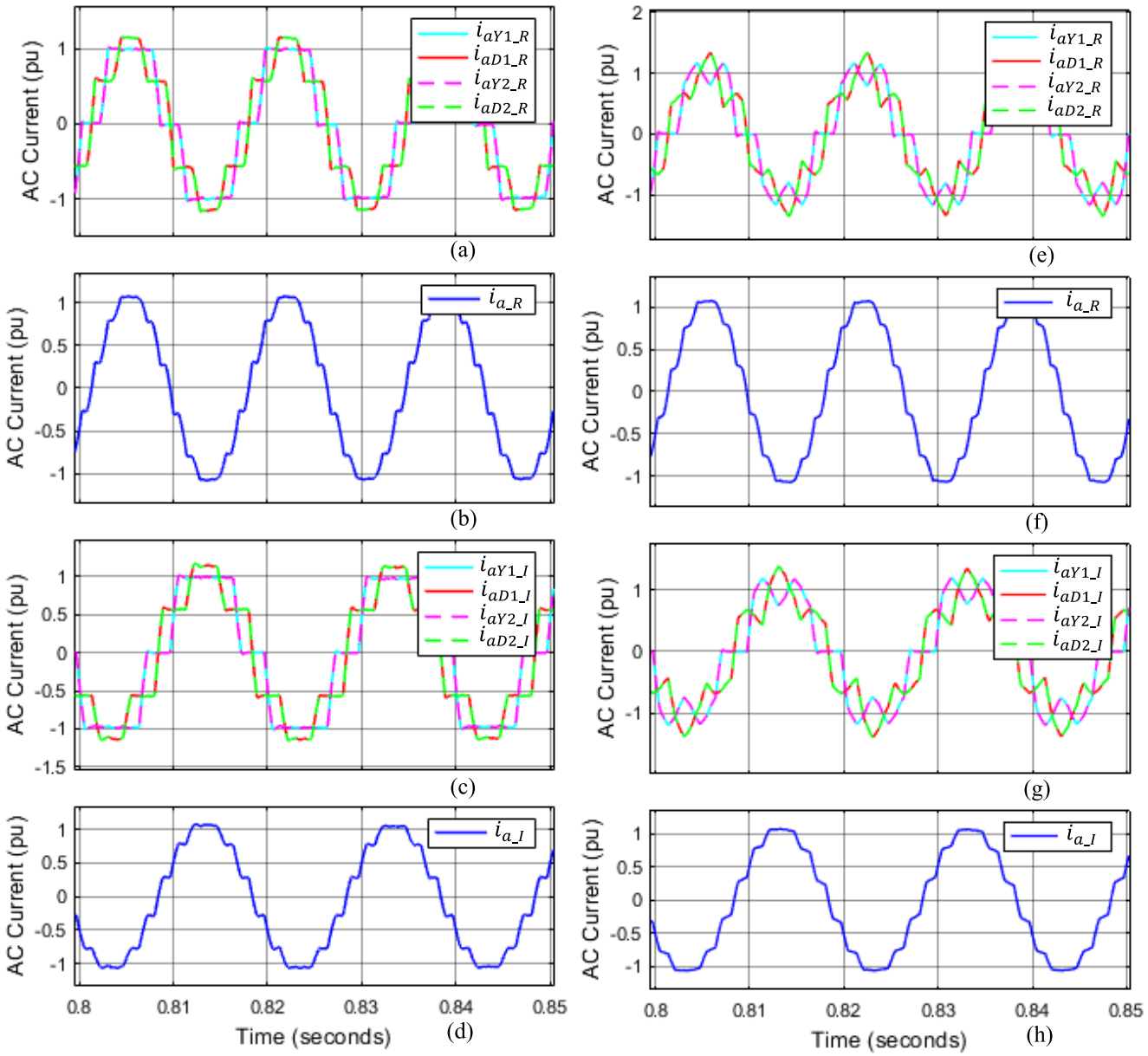

FIGURE 6. Waveform of the phase current i_a for the conventional 2PBTBS and the proposed 4PBTBS: (a) at each transformer of the rectifier side in the 2PBTBS, (b) at AC system 1 in the 2PBTBS, (c) at each transformer of the inverter side in the 2PBTBS, (d) at AC system 2 in the 2PBTBS, (e) at each transformer of the rectifier side in the 4PBTBS, (f) at AC system 1 in the 4PBTBS, (g) at each transformer of the inverter side in the 4PBTBS, (h) at AC system 2 in the 4PBTBS.

B. SIMULATION RESULTS

Fig. 6 shows the results of the waveform of the AC line currents at phase *a* of the primary winding of each converter transformer for the conventional 2PBTBS and the proposed 4PBTBS, respectively. The waveforms of AC currents i_{aY1_R}, i_{aD1_R}, i_{aY2_R}, i_{aD2_R} and i_{aY1_I}, i_{aD1_I}, i_{aY2_I}, i_{aD2_I} are measured at the primary winding of the rectifier and inverter transformers of the 2PBTBS, as depicted in Figs. 6(a) and (c), respectively. Fig. 6(b and d) shows the total AC currents at bus bar B_{rec} at the rectifier side and B_{inv} at the inverter side, respectively (see Fig. 3(a)).

Furthermore, the waveforms of AC currents i_{aY1_R}, i_{aD1_R}, i_{aY2_R}, i_{aD2_R} and i_{aY1_I}, i_{aD1_I}, i_{aY2_I}, i_{aD2_I} are measured at primary winding of the rectifier and inverter transformers of 4PBTBS, as depicted in Fig. 6(e and g), respectively. Fig. 6(f and h) shows the total AC currents at bus bars B_{rec} at the rectifier side and B_{inv} at the inverter side, respectively (Fig. 3(b)).

Comparing Figs. 6(a)–6(d) with Figs. 6(e)–6(h) can easily notice the distinguished effect of the proposed 4PBTBS topology on the total AC currents at bus-bars B_{rec} and B_{inv} at the rectifier and inverter sides. The simulation results of the

TABLE 6. Relation between harmonic orders and harmonic at AC line currents of rectifier and inverter sides for 2PBTBS & 4PBTBS.

h	2PBTBS		4PBTBS	
	Rate of Harmonics I_h/I_d (%) at AC system 1	Rate of Harmonics I_h/I_d (%) at AC system 2	Rate of Harmonics I_h/I_d (%) at AC system 1	Rate of Harmonics I_h/I_d (%) at AC system 2
I_d	100	100	100	100
2	0.20	0.12	0.10	0.16
3	0.31	0.31	0.04	0.37
4	0.11	0.13	0.20	0.08
5	0.11	0.09	0.04	0.29
6	0.07	0.21	0.08	0.03
7	0.12	0.06	0.02	0.16
8	0.15	0.20	0.06	0.02
9	0.22	0.29	0.11	0.16
10	0.11	0.16	0.01	0.08
11	5.54	6.45	4.67	5.30
12	0.08	0.15	0.06	0.04
13	3.88	4.97	3.31	4.08
14	0.23	0.26	0.08	0.18
15	0.12	0.17	0.05	0.12
16	0.07	0.07	0.06	0.04
17	0.10	0.04	0.04	0.05
18	0.06	0.07	0.06	0.03
19	0.18	0.03	0.18	0.15
20	0.08	0.07	0.08	0.03
21	0.21	0.04	0.21	0.13
22	0.11	0.03	0.11	0.02
23	0.85	0.27	0.85	0.74
24	0.03	0.01	0.03	0.04
25	0.70	0.33	0.70	0.53
THD	**6.90%**	**8.22%**	**5.82%**	**6.81%**

THD at AC systems 1 and 2 for the 2PBTBS and 4PBTBS are shown in Table 5. Although both systems use the same AC filter capacities, the THD is reduced in the proposed 4PBTBS in comparison with the conventional 2PBTBS. Therefore, the AC currents at AC sides of the proposed 4PBTBS HVDC converter meet the power quality standard requirement determined by the IEEE Standard (IEEE Std 519).

V. RELIABILITY EVALUATION OF THE PROPOSED SYSTEM

In accordance to loop currents 1 and 2 in Fig. 2(a) for the 2PBTBS and loop currents 1, 2, 3, and 4 in Fig. 2(b) for the 4PBTBS, each loop current in the 2PBTBS and 4PBTBS is capable of 50% and 25% of the original system capacity, respectively.

The reliability of the HVDC system can be determined by making the following assumptions [4], [19]:

1) Each 12-pulse HVDC circuit in the 2PBTBS and 4PBTBSS has the same components and capable of 50% of the original system capacity.
2) The reliability of one 12-pulse HVDC circuit in the proposed 4PBTBS is almost equal to that of one 12-pulse HVDC circuit in the conventional 2PBTBS.
3) The failure of one or more series-dependent components in the 12-pulse HVDC circuit results in a complete failure of the circuit.
4) The failure of one or more parallel-dependent components (common components) in the 12-pulse HVDC circuit may not result in a circuit failure but may limit the system capacity.

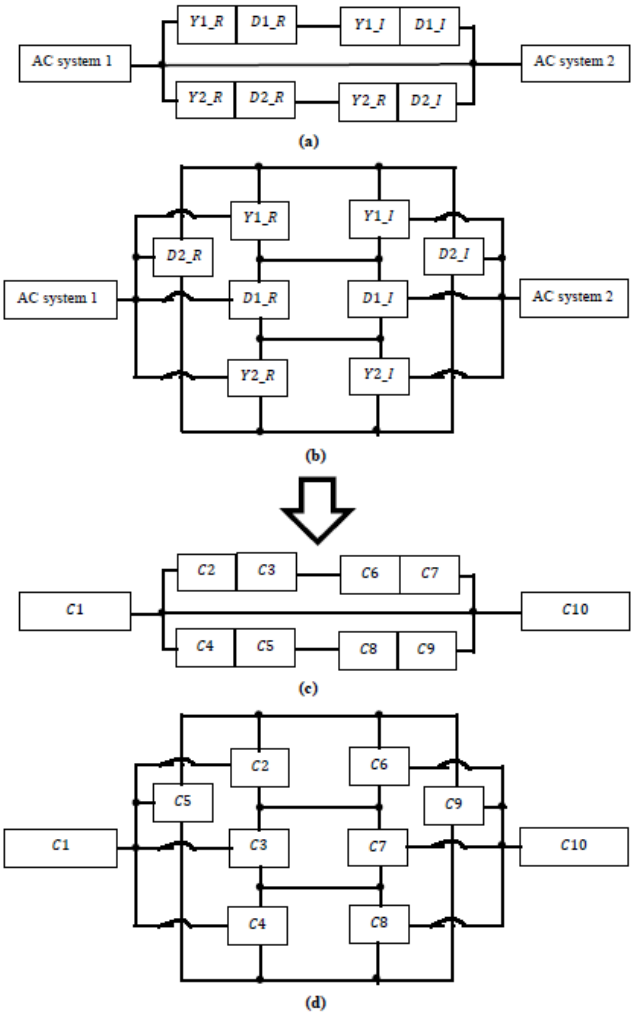

FIGURE 7. Reliability logic diagram and components capacities of, (a) and (c) existing 2PBTBS, (b) and (d) proposed 4PBTBS, respectively.

Fig. 7(a and b) shows the reliability logic diagram for the 2PBTBS and 4PBTBS, respectively. The reliability diagrams of 2PBTBS and 4PBTBS are built by combining between Fig. 2(a and b) and the failure effects of the 12-pulse DC circuits as shown in Tables 1 and 2. Fig. 7(c and d) illustrates the capacity of various components in each 12-pulse DC circuit for the 2PBTBS and 4PBTBS translated from Fig. 7(a and b), respectively.

The capacity is indicated as $Ci\,(i = 1, 2, \ldots, m)$, where $m = 10$ for Fig. 7(c and d), respectively. Therefore, the capacity of the whole system of the 2PBTBS and 4PBTBS can be

determined using Equations (12) and (13), correspondingly.

$$C_{2PBTBS} = C1[(C2.C3.C6.C7)] + (C4 \cdot C5 \cdot C8 \cdot C9)\, C10 \quad (12)$$

$$C_{4PBTBS} = C1[(C2.C6) + (C3 \cdot C7) + (C4 \cdot C8) + (C5 \cdot C9)]C10 \quad (13)$$

where, C_{2PBTBS} and C_{4PBTBS} are the available capacities of the 2PBTBS and 4PBTBS, respectively. In Equation (12), $C1 = C10 = 100\%$ of the system capacity, whereas $C2 = C3 = C4 = C5 = C6 = C7 = C8 = C9 = 50\%$ of the system capacity. However, in Equation (13), $C1 = C10 = 100\%$ in the system capacity, and $C2 = C3 = C4 = C5 = C6 = C7 = C8 = C9 = 25\%$ of the system capacity.

For example, two 6-pulse inverter bridges $Y1\_R$ and $D2\_R$ in the 2PBTBS and 4PBTBS are down simultaneously, whereas all other components are in a normal state. In the 2PBTBS and 4PBTBS, the 6-pulse bridges $Y1\_R$ and $D2\_R$ represent capacities $C2$ and $C5$, respectively. The values of the capacities $C2$, $C5$ for the 2PBTBS and 4PBTBS are zero. By substituting the values of $C2$ and $C5$ into Equations (12) and (13), the transfer capacity of the whole 2PBTBS is 0, whereas that of the 4PBTBS is 50%.

Aside from the relatively lower voltage levels and the use of four effective 12-pulse converter units at the rectifier and inverter sides in the proposed 4PBTBS, the 4PBTBS topology is equivalent to the four parallel 2PBTBS topologies. These effective parallel 12-pulse circuits and the outage effects of each component on the system reliability performance for the 2PBTBS and 4PBTBS are shown in Figs. 8 and 9, respectively.

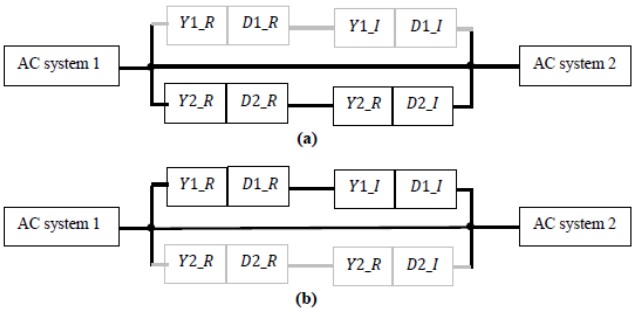

FIGURE 8. Mono-Pole Outages in the existing 2PBTBS (Grey colour), (a) Pole 1 outage, (b) Pole 2 outage.

Fig. 8(a and b) shows all six-pulse bridges in the 12-pulse DC circuits 1 and 2 are the series-dependent components. For example, the bridge $Y1\_R$ outage results in a mono-pole outage (pole 1) as shown in Fig. 8(a). Fig. 8(b) shows the pole 2 outage because one of the 6-pulse bridges in this pole is down.

Fig. 9(a to d) shows that all six-pulse bridges in the 12-pulse DC circuits 1, 2, 3, and 4 are the parallel dependent components. For example, the bridge $Y1\_R$ and $D1\_R$ outages in Fig. 9(a) result in a bi-pole outage (poles 1 and 2)

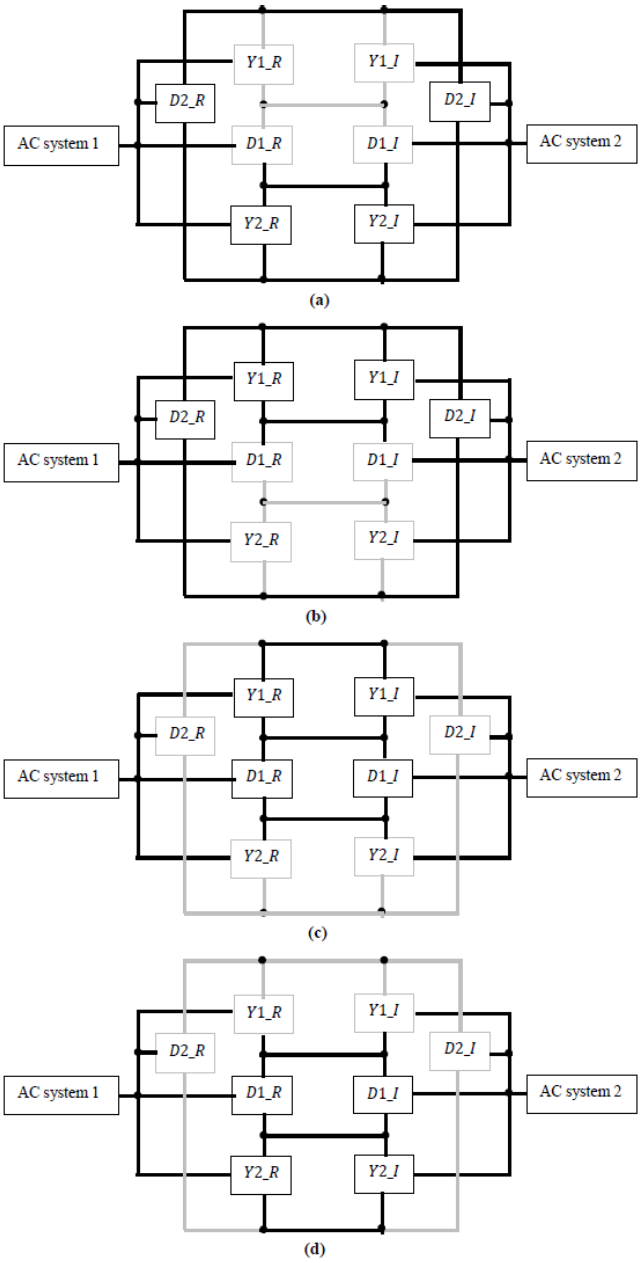

FIGURE 9. Bi-Pole Outages in the proposed 4PBTBS (Grey colour), (a) Poles 1 & 2 outage, (b) Poles 2 & 3 outage, (c) Poles 3 & 4 outage, (d) Poles 4 & 1 outage.

and allow the healthy poles (poles 3 and 4) of the 4PBTBS to operate as a typical bi-pole HVDC system capable of 50% of the total system capacity. Similarly, poles 2 and 3 outages cause 50% the system loses of its capacity, as shown in Fig. 9(b); poles 3 and 4 outages cause 50% the system loses of its capacity, as shown in Fig. 9(c); poles 4 and 1 outages cause 50% the system loses of its capacity, as shown in Fig. 9(d).

The outage effects of each component (six-pulse bridge) on the conventional 2PBTBS reliability performance can be categorized into series-dependent components. Meanwhile, the outage effects of each component (six-pulse bridge)

TABLE 7. Cost and performance comparison results between the existing 2PBTBS and proposed 4PBTBS.

	2PB TBS	4PB TBS
Number of 6-pulse converter units (6-pulse thyristor bridge and transformer) required per system	8	8
Number of short bus-bar required per system	4	4
AC filters capacity at rectifier side (in $p.u.$)	1	1
AC filters capacity at inverter side (in $p.u.$)	1	1
DC current value per 6-pulse bridge unit (in $p.u.$)	1	1
Power losses per 6-pulse bridge unit (in $p.u.$)	1	1
Maximum power capacity per 6-pulse DC circuit (in $p.u.$)	0.25	0.25
Maximum power capacity per 12-pulse DC circuit (in $p.u.$)	0.5	0.25
Maximum power capacity per system (in $p.u.$)	1	1

on the proposed 4PBTBS reliability performance can be categorized into parallel dependency components (common components). This setup provides four effective parallel independent 12-pulse DC circuits instead of only two as in the existing 2PBTBS. The reliability of the one 12-pulse DC circuit in the existing 2PBTBS is equal to that in the proposed 4PBTBS. Therefore, increasing the number of parallel 12-pulse DC circuits in the proposed 4PBTBS increases reliability. As a result, the reliability of the proposed 4PBTBS topology has improved approximately twice over the existing 2PBTBS.

VI. DISCUSSION

Basically, a typical 12-pulse HVDC system has the same components and parameters at the rectifier and inverter sides [4]. Therefore, the existing 2PBTBS can be upgraded to the new 4PBTBS HVDC converter without additional cost (Table 7). The success of upgrading the existing 2PBTBS to the new 4PBTBS HVDC converter is defined by mathematical and simulation results. The cost and performance comparison results between the existing 2PBTBS and the proposed 4PBTBS are summarized in Table 7.

The 2PBTBS and 4PBTBS topologies have the same components, as shown in Fig. 1(a and b), respectively. The existing 2PBTBS topology can produce only two 12-pulse DC circuits. Each circuit is capable of 50% of the total capacity of the 2PBTBS. The proposed 4PBTBS topology can produce four 12-pulse DC circuits with relatively low DC voltage levels. Each circuit is capable of 50% of the total capacity of the 4PBTBS. The reliability of a single 12-pulse DC circuit in the proposed 4PBTBS is almost equal to that of a single 12-pulse DC circuit in the existing 2PBTBS. Therefore, the 4PBTBS topology has six operating modes (Table 2) instead of only four as in the existing 2PBTBS topology (Table 1). As a result, the system reliability of the proposed 4PBTBS topology is improved approximately twice in comparison with the existing 2PBTBS topology.

VII. CONCLUSION

A novel topology has been proposed and successfully applied to BTBS LCC-HVDC for upgrading the existing 2PBTBS with two parallel 12-pulse DC circuits into the 4PBTBS with four parallel 12-pulse DC circuits. The 2PBTBSs are used for importing or exporting electrical energy between two asynchronous AC systems. These AC systems can be with the same or different frequency. The advantages of upgrading the existing 2PBTBS to the proposed 4PBTBS can be summarized as follows:

1) System reliability in the proposed 4PBTBS is approximately two times higher than that in the existing 2PBTBS.
2) Although the 2PBTBS and 4PBTBS topologies are using the same 6-pulse bridge units with the same parameters, the proposed 4PBTBS topology can reduce the line-to-line DC voltage levels by 50% over the existing 2PBTBS.
3) Although the 2PBTBS and 4PBTBS have the same AC filter capacities at AC system 1 and 2 sides of the BTBS, the THD values of the AC line currents of the proposed 4PBTBS reduce by approximately 1.08% and 1.41%, respectively, in comparison with the existing 2PBTBS.
4) Although the 2PBTBS and 4PBTBS have different topologies, they have the same components and parameters. Therefore, the existing 2PBTBS can be upgraded to the new 4PBTBS HVDC converter without additional cost.

REFERENCES

[1] S. R. Mohammed, J. Teh, and M. K. M. Jamil, "A novel quad 12-pulse four-pole system using an existing 12-pulse bi-pole system for back-to-back HVDC system," in *Proc. IEEE PES Asia–Pacific Power Energy Eng. Conf. (APPEEC)*, Kota Kinabalu, Malaysia, Oct. 2018, pp. 325–330.
[2] *IEEE Guide for Specification of High-Voltage Direct-Current Systems. Part I—Steady-State Performance*, IEEE Standard 1030, 1987.
[3] A. G. Siemens. (2011). High Voltage Direct Current Transmission–Proven Technology for Power Exchange. Siemens. Erlangen, Germany. [Online]. Available: https://www.energy.siemens.com/hq/pool/hq/power-transmission/HVDC/HVDC_Proven_Technology.pdf
[4] C.-K. Kim, V. K. Sood, G.-S. Jag, S.-J. Lim, and S.-J. Lee, *HVDC Transmission: Power Conversion Applications in Power Systems*. Singapore: Wiley, 2009.
[5] A. E. Hammad and W. F. Long, "Performance and economic comparisons between point-to-point HVDC transmission and hybrid back-to-back HVDC/AC transmission," *IEEE Trans. Power Del.*, vol. 5, no. 2, pp. 1137–1144, Apr. 1990. doi: 10.1109/61.53132.
[6] C. Saldaña and G. Calzolari, "Modelling of the 500 MW back-to-back converter station between uruguay and Brazil in ATP," in *Proc. AEIT HVDC Int. Conf.*, Florence, Italy, May 2019, pp. 1–6.
[7] A. G. Siemens. (2011). HVDC-High Voltage Direct Current Power Transmission Unrivalled Practical Experience. Siemens. Erlangen, Germany. [Online]. Available: https://www.energy.siemens.com/br/pool/hq/power-transmission/HVDC/HVDC-Classic/HVDC-Classic_Transmission_References_en.pdf
[8] Q. Nguyen, G. Todeschini, and S. Santoso, "Power flow in a multi-frequency HVAC and HVDC system: Formulation, solution, and validation," *IEEE Trans. Power Syst.*, vol. 34, no. 4, pp. 2487–2497, Jul. 2019. doi: 10.1109/TPWRS.2019.2896023.
[9] T. Yoshino, "History and trends of converter technology for DC and AC transmission in Japan," in *Proc. Int. Power Electron. Conf.*, Hiroshima, Japan, May 2014, pp. 3834–3841.

[10] T. Sakai, Y. Makino, and H. Kosaka, "Technologies applied to Japan's HVDC links," CIGRE.org, Thailand, Rep. AORC Tech. Meeting, 2014. [Online]. Available: https://www.cigre-thailand.org/tncf/events/aorc2014/full_paper/1073R.pdf
[11] L. E. Juhlin, G. Liss, and A. Ekstrom, "Parallel connection of convertors for HVDC transmission," *IEEE Trans. Power App. Syst.*, vols. PAS–97, no. 3, pp. 714–724, May 1978. doi: 10.1109/TPAS.1978.354542.
[12] H. Bilodeau, S. Babaei, B. Bisewski, J. Burroughs, C. Drover, J. Fenn, B. Fardanesh, B. Tozer, B. Shperling, and P. Zanchette, "Making old new again: HVdc and FACTS in the northeastern United States and Canada," *IEEE Power Energy Mag.*, vol. 14, no. 2, pp. 42–56, Mar./Apr. 2016.
[13] Z. Eugeny, N. Lozinova, O. Suslova, M. Andreev, R. Ufa, N. Ruban, and A. Suvorov, "HVDC LCC technology and power quality issues in cross-border electrical power transmission Russia–Finland," in *Proc. IEEE PES Innov. Smart Grid Technol. Conf. Eur. (ISGT-Eur.)*, Sarajevo, Bosnia-Herzegovina, Oct. 2018, pp. 1–6.
[14] R. Hibberts-Caswell, L. Oprea, and M. Salimi, "Design considerations for an HVDC VSC Back-to-Back converter in parallel operation with HVDC LCC back-to-back converter," in *Proc. VDE High Voltage Technol. Conf. (ETG-Symp.)*, Berlin, Germany, 2018, pp. 752–755.
[15] S. R. Mohammed, J. Teh, and M. K. M. Jamil, "Reliability and power density increase in a novel four-pole system for line-commutated converter HVDC transmission," *IEEE Access*, vol. 7, pp. 10057–10076, 2019. doi: 10.1109/ACCESS.2019.2891780.
[16] B. M. Weedy, B. J. Cory, N. Jenkins, J. B. Ekanayake, and G. Streak, *Electric Power Systems*, 5th ed. Chichester, U.K.: Wiley, 2012, pp. 319–353.
[17] G. Sybille, L.-A. Dessaint, B. Dekelper, O. Tremblay, J.-R. Cossa, P. Brunelle, R. Champagne, P. Giroux, R. Gagnon, S. Casoria, H. Lehuy, H. Fortin-Blanchette, O. Tremblay, C. Semaille, H. Ouquelle, J.-N. Paquin, and P. Mercier, "Thyristor-based HVDC link," in *SimPowerSystemsTM User's Guide, SimPowerSystemsTM Software R2013a* (Hydro-Quebec and The Math Works), 2013, pp. 5.39–5.60.
[18] *IEEE Recommended Practice and Requirements for Harmonic Control in Electric Power Systems*, IEEE Standard 519, 2014.
[19] R. Billinton and R. N. Allan, *Reliability Evaluation of Engineering Systems: Concepts and Techniques*, 2nd ed. New York, NY, USA: Plenum Press, 1992, pp. 81–100.

SABAH RAMADHAN MOHAMMED received the B.Eng. degree from Northern Technical University, Nineveh, Iraq, and the M.Sc. degree from Universiti Teknikal Malaysia, Melaka (UTeM), Melaka, Malaysia, in 2014, both in electronic and computer engineering, and the Ph.D. degree in electrical and electronic engineering from Universiti Sains Malaysia (USM), Penang, Malaysia, in 2019.

His research interests include power systems and energy conversion.

JIASHEN TEH (M'17) received the B.Eng. degree in electrical and electronic engineering from Universiti Tenaga Nasional (UNITEN), Selangor, Malaysia, in 2010, and the Ph.D. degree in similar field from The University of Manchester, Manchester, U.K., in 2016.

He is currently a Senior Lecturer with the Universiti Sains Malaysia (USM), Penang, Malaysia. His research interests include power system reliability analyses, renewable energy sources, and smart grid technologies. He is a Chartered Engineer, a member of the IET, and a registered graduate engineers Malaysia (BEM) in the electrical track.

MOHAMAD KAMAROL (M'10–SM'19) received the B.Eng. (Hons.) degree in electrical engineering from Universiti Technology Mara, Malaysia (UiTM), in 2000, the M.Eng. degree from the Kyushu Institute of Technology, Japan, in March 2005, and the D.Eng. degree, in March 2008. He joined Universiti Sains Malaysia (USM) with a University ASTS Fellowship, in 2002. Within his doctor course study, he has received the Chatterton Young Investigator Award from the IEEE International Symposia on Discharges and Electrical Insulation in Vacuum (ISDEIV), in 2006. Prior to joining the university, he worked as a Senior Engineer with the Sankyo Seiki (M) Sdn. Bhd., for almost eight years. He was a Visiting Researcher with the High Voltage Laboratory, Kyushu Institute of Technology, Japan, from 2013 to 2014. He was a Senior Lecturer with USM, Malaysia, since 2008, and has been promoted to Associate Professor at the same university, in December 2014. His research interests include the insulation properties in oil palm and solid dielectric material, insulation properties of environmentally benign gas, and PD detection technique for insulation diagnosis of power apparatus and electrical machine. He is also involved in temperature rise and short circuit electromagnetic study of busbar system and HVDC system. He is a Professional Engineer, a Chartered Engineer, and a member of the IET, the Board of Engineering Malaysia (BEM), and the Institute Engineering Malaysia (IEM).